Envelope-Finite-Element (EVFE) Technique—A More Efficient Time-Domain Scheme

Yuanxun Wang, *Member, IEEE,* and Tatsuo Itoh, *Fellow, IEEE*

***Abstract*—A novel technique, called the envelope-finite element (EVFE) method, is proposed as a more efficient full-wave time-domain modeling scheme of electromagnetic waves. The EVFE method simulates the signal envelope rather than the original signal waveform by de-embedding the signal carrier from the time-domain wave equation. The de-embedded equation is then solved in the time domain using finite-element methods based on Newmark–Beta time stepping. Compared to traditional time-domain simulation techniques such as finite difference time-domain or finite element time-domain methods, only the signal envelope needs to be sampled in EVFE simulation. This method can reduce computation time when signal envelope/carrier ratios are very small. The purpose of this paper is to introduce this new concept, by presenting the two-dimensional EVFE formulations, stability conditions, and some supporting numerical examples.**

***Index Terms*—Envelope simulation, finite-element method, full-wave approach, time-domain modeling.**

I. Introduction

TRADITIONAL electromagnetic transient simulation techniques such as finite-difference time-domain (FDTD) methods or finite-element time-domain (FETD) methods have become quite popular for the past two decades. Compared to their frequency-domain analogy, their capability to generate time-domain waveforms in a straightforward manner bring many advantages in simulating broad-band system responses or identifying circuit parasitics [1], [2]. There are also efforts on time-domain co-simulations coupling electromagnetic waves with active/nonlinear devices [3], [4]. However, the time step in simulation is usually required to be very small because of the CFL stability condition. Even when their implicit versions [5], [6] are used, the time-domain waveform has to be sampled at a minimum of twice the highest signal frequency to satisfy the Nyquist sampling criterion regardless of the signal bandwidth.

However, modern wireless and optical communication signals often employ digital modulations on the RF carriers or RF modulations on the optical carriers. The signal bandwidths in these systems are usually very narrow relative to their carrier frequencies. When transient simulators are used for this case, much of the computation is wasted. To address this limitation, a new circuit simulation technique called the Circuit Envelope has been recently introduced in [7] and exploited in HPEEsof's ADS or MDS design software. By discretizing and simulating the signal envelopes on defined carrier frequencies, it has proven to be much more efficient than transient simulators like SPICE for narrow-band cases.

Based on a the similar concept, a novel electromagnetic solver called the envelope-finite element (EVFE) technique is proposed in this paper. Derived rigorously from Maxwell's equations, the EVFE technique is able to simulate time-varying complex envelopes of electromagnetic waves. The essential idea is to perform time marching of the signal envelope on top of the frequency-domain finite-element method (FEM) solution at the carrier frequency. This is achieved by de-embedding the signal carrier from the time-domain wave equation, on which the FEM is based. Since only the signal envelope needs to be sampled, much sparser time steps can be used than those in FDTD or FETD techniques, which results in much higher computation efficiency when the envelope/carrier ratio is small. In addition to all the advantages as a full-wave time-domain technique, EVFE techniques also have considerable computational advantages over frequency-domain FEM, because there is no need to solve the boundary value problem once again for each different frequency. The inversion of the finite element matrix only needs to be done once for the defined carrier frequency, if a direct solver is used. Even for large-scale three-dimensional (3-D) problems where an iterative solver is necessary, the matrix formation and precondition for a different frequency need not be repeated. The algorithm is also of low complexity and can be easily written by modifying a conventional FEM code.

This paper is organized as follows. The EVFE formulations are first derived from the scalar wave equations in Section II. The proof of unconditional stability in time-domain recurrence is then given in Section III. In Section IV, the dispersion error of the proposed approach is analyzed numerically by studying a two-dimensional (2-D) cavity with regarding to different time-step and carrier frequency selection. Section V presents the implementation of traveling wave boundary conditions for EVFE formulation. For validation, EVFE solutions of some guided-wave problems are obtained in Section VI, with comparison to frequency-domain FEM solutions. Finally, the conclusion of this paper is given in Section VII.

II. EVFE Formulations

For simplicity, the EVFE formulation presented here is only for 2-D TEM or TM waves [8]. It can be easily extended for 3-D full-vector modeling of arbitrary microwave structures. The time-dependent electromagnetic field excited by electric current

Manuscript received March 31, 2001; revised August 17, 2001.

The authors are with the Department of Electrical Engineering, University of California at Los Angeles, Los Angeles, CA 90095-1594 USA (e-mail: itoh@ee.ucla.edu).

Publisher Item Identifier S 0018-9480(01)10472-2.

density $\vec{J}$ is described by the following inhomogeneous wave equation:

$$\nabla \times \left(\frac{1}{\varepsilon}\nabla \times \vec{H}\right) + \sigma\frac{\mu}{\varepsilon}\frac{\partial \vec{H}}{\partial t} + \mu\frac{\partial^2 \vec{H}}{\partial t^2} = \frac{1}{\varepsilon}\nabla \times \vec{J} \quad (1)$$

where σ is the conductivity, $\varepsilon = \varepsilon_r\varepsilon_0$ and $\mu = \mu_r\mu_0$ are, respectively, the permittivity and permeability. For a 2-D area S is bound by the boundary Γ, it follows that the scalar wave equation regarding to longitudinal component of magnetic field is

$$\frac{1}{\varepsilon_r\varepsilon_0}\nabla^2 H_z - \sigma\frac{\mu_r\mu_0}{\varepsilon_r\varepsilon_0}\frac{\partial H_z}{\partial t} - \mu_r\mu_0\frac{\partial^2 H_z}{\partial t^2} = -\frac{1}{\varepsilon_r\varepsilon_0}\left(\nabla \times \bar{J}\right)_z \quad (2)$$

where ε_r and μ_r are the relative permittivity and permeability. By defining the carrier frequency ω_c, the field component and the current density can be written in a modulated signal format as

$$\begin{aligned} H_z(t) &= V(t)e^{j\omega_c t} \\ \vec{J}(t) &= \vec{j}(t)e^{j\omega_c t} \end{aligned} \quad (3)$$

where $V(t)$ is the time-varying complex envelope of the field at the carrier frequency. It should be noted that the expression in (3) is not unique but dependent on the definition of carrier frequency. Normally the carrier is chosen to be the center frequency of the interested frequency band in order to minimize the envelope frequency. Substituting (3) into (2) and dividing both sides by $e^{j\omega_c t}$ yields the partial differential equation (PDE) for the envelope

$$\frac{1}{\varepsilon_r}\nabla^2 V(t) + \frac{\mu_r}{c_0^2}\left[(\omega_c^2 - j\alpha\omega_c) - (\alpha + 2j\omega_c)\frac{\partial}{\partial t} - \frac{\partial}{\partial t^2}\right]\cdot V(t) = -\frac{1}{\varepsilon_r}\left(\nabla \times \vec{j}\right)_z \quad (4)$$

where c_0 is the free-space light speed and $\alpha = \sigma/\varepsilon_r\varepsilon_0$ is a constant. Let's call (4) an envelope equation. It is noticed that the envelope equation reduces to a scalar Helmholtz equation when V is time independent, on which the frequency-domain FEM is based. On the other hand, if the carrier frequency ω_c is chosen to be zero, the envelope equation is also equivalent to the time-dependent wave equation on which the implicit FETD method is based. Therefore, one can easily solve it by treating it as the other time-dependent wave equations. The inner product of (4) with a testing function T leads to the weak form

$$\begin{aligned} \iint_s \Bigg[\frac{1}{\varepsilon_r}\nabla T \cdot \nabla V - \frac{\mu_r}{c_0^2} \cdot \left[(\omega_c^2 - j\alpha\omega_c) - (\alpha + 2j\omega_c)\frac{\partial}{\partial t} - \frac{\partial}{\partial t^2}\right]\cdot T \cdot V\Bigg]\cdot ds \\ = \iint_s \frac{1}{\varepsilon_r} T \cdot \left(\nabla \times \vec{j}\right)_z \cdot ds + \oint_\Gamma \frac{1}{\varepsilon_r} T\frac{\partial V}{\partial n}\cdot dl. \end{aligned} \quad (5)$$

Assuming that the boundary Γ consists of only perfect electric conductor (PEC) or perfect magnetic conductor (PMC), the path integral term on the right-hand side vanishes. For spatial discretization, the envelope variable is expanded in terms of 2-D FEM basis functions W_j. The application of Galerkin's process results in a system of ordinary differential equations

$$\mathbf{T}\frac{d^2 v}{dt^2} + \mathbf{B}\frac{dv}{dt} + \mathbf{S}v + \mathbf{F} = 0 \quad (6)$$

where v is the coefficient vector of V. $\mathbf{T}$, $\mathbf{B}$, and $\mathbf{S}$ are time-independent matrices and are defined by

$$\begin{aligned} T_{ij} &= \iint_s \frac{\mu_r}{c_0^2} W_i W_j\, ds \\ B_{ij} &= \iint_s \frac{\mu_r}{c_0^2}(2j\omega_c + \alpha)\cdot W_i W_j\, ds \\ S_{ij} &= \iint_s \frac{1}{\varepsilon_r}\nabla W_i \cdot \nabla W_j - \frac{\mu_r}{c_0^2}(\omega_c^2 - j\alpha\omega_c)\cdot W_i W_j\, ds \\ Fi &= \iint_s \frac{1}{\varepsilon_r} W_i \cdot \left(\nabla \times \bar{j}\right)_z ds. \end{aligned} \quad (7)$$

To discretize (7) in the time domain, the Newmark–Beta formulation [6] can be used

$$\begin{cases} \dfrac{d^2 v}{dt^2} = \dfrac{1}{\Delta t^2}\left[v(n+1) - 2v(n) + v(n-1)\right] \\ \dfrac{dv}{dt} = \dfrac{1}{2\Delta t}\left[v(n+1) - v(n-1)\right] \\ v = \beta v(n+1) + (1-2\beta)v(n) + \beta v(n-1) \end{cases} \quad (8)$$

where $v(n) = v(n\Delta t)$ is the discrete-time representation of $v(t)$. β is a constant that has to be carefully chosen to guarantee stability. It is recommended that $\beta = 1/4$, which leads to an unconditionally stable two-step update scheme as we shall prove next. Therefore, the resulted update scheme is

$$\begin{aligned} &\left[\frac{\mathbf{T}}{\Delta t^2} + \frac{\mathbf{B}}{2\Delta t} + \frac{\mathbf{S}}{4}\right]v(n+1) \\ &= \left[\frac{2\mathbf{T}}{\Delta t^2} - \frac{\mathbf{S}}{2}\right]v(n) + \left[-\frac{\mathbf{T}}{\Delta t^2} + \frac{\mathbf{B}}{2\Delta t} - \frac{\mathbf{S}}{4}\right]v(n-1) - f(n). \end{aligned} \quad (9)$$

To solve the above equations, the matrix on the left-hand side needs to be inversed. Note that this matrix is time independent: it needs to be filled and solved only once if a direct sparse-matrix solver is used.

III. Stability Analysis

The stability analysis of FETD methods has been presented in both [5] and [6]. Here the stability condition for EVFE techniques will be derived in a way similar to the work in [6]. However, as we shall find out, the derived stability condition for EVFE techniques is not exactly the same as that in FETD methods. Assuming there is no excitation in the system given

in (6), the stability can be examined with regarding to the following differential equations:

$$\mathbf{T}\frac{d^2v_m}{dt^2}+\mathbf{B}\frac{dv_m}{dt}+\mathbf{S}v_m=0 \tag{10}$$

where v_m is the mth solution vector of the above homogeneous equations, e.g., the field envelope vector for the mth mode. After the discretization in time, the two-step recurrence algorithm for $v(n)$ takes the form

$$\begin{aligned}&\left[\mathbf{T}+\frac{1}{2}\Delta t\mathbf{B}+\Delta t^2\beta\mathbf{S}\right]v_m(n+1)\\&\quad+\left[-2\mathbf{T}-\Delta t^2(2\beta-1)\mathbf{S}\right]v_m(n)\\&\quad+\left[\mathbf{T}-\frac{1}{2}\Delta t\mathbf{B}+\Delta t^2\beta\mathbf{S}\right]v_m(n-1)=0.\end{aligned} \tag{11}$$

The general solution can be written as

$$\begin{aligned}v_m(n+1)&=\lambda_m^2v(n-1)\\v_m(n)&=\lambda_mv(n-1)\end{aligned} \tag{12}$$

where λ_m is the growth factor for mode m, which is a scalar number. Substituting (12) into (11) yields the following equation:

$$\mathbf{A}(\lambda_m)v_m=0 \tag{13}$$

where $\mathbf{A}(\lambda_m)$ is the second-order characteristic matrix polynomial for λ_m [9]. It takes the form

$$\begin{aligned}\mathbf{A}(\lambda_m)=&\left[\mathbf{T}+\frac{1}{2}\Delta t\mathbf{B}+\Delta t^2\beta\mathbf{S}\right]\lambda_m^2\\&+\left[-2\mathbf{T}-\Delta t^2(2\beta-1)\mathbf{S}\right]\lambda_m\\&+\left[\mathbf{T}-\frac{1}{2}\Delta t\mathbf{B}+\Delta t^2\beta\mathbf{S}\right].\end{aligned} \tag{14}$$

Therefore, the growth factor λ_m and mode vector v_m are, respectively, the mth eigen value and eigen vector of the second-order eigen value problem represented by (13). Taking the inner product of (13) with regarding to the mode vector v_m, it follows that

$$\langle\mathbf{A}(\lambda_m)v_m,\,v_m\rangle=v_m^H\mathbf{A}(\lambda_m)v_m=0. \tag{15}$$

Let T_m, B_m, and S_m represent, respectively, the inner products of $\mathbf{T}$, $\mathbf{B}$, and $\mathbf{S}$ with regard to v_m. Equation (15) reduces to a set of scalar second-order equations as follows:

$$\begin{aligned}&\left[T_m+\frac{1}{2}\Delta tB_m+\Delta t^2\beta S_m\right]\lambda_m^2\\&\quad+\left[-2T_m-\Delta t^2(2\beta-1)S_m\right]\lambda_m\\&\quad+\left[T_m-\frac{1}{2}\Delta tB_m+\Delta t^2\beta S_m\right]=0.\end{aligned} \tag{16}$$

For stability, it is necessary that the modulus of the growth factor be bounded by one for all modes, e.g., $|\lambda_m|\le 1,\ \forall\, m$. Therefore, it has to be shown that all the roots of the above equations are within the unit circle. It is well known that the interior of the unit circle is mapped to the left-half plane under the so-called z transform. Therefore, let

$$\lambda_m=\frac{1+z_m}{1-z_m}. \tag{17}$$

Equation (16) is now rewritten in terms of z as

$$\left[(4T_m+\Delta t^2(4\beta-1)S_m\right]z_m^2+2\Delta tB_mz_m+\Delta t^2S_m=0. \tag{18}$$

The stability requirement is thus equivalent to demanding the real part of z_m to be nonpositive. The roots of the above second-order equation are well known as

$$z_m=\frac{-b\pm\sqrt{b^2-4ac}}{2a} \tag{19}$$

where a, b, and c are polynomial coefficients in (18). In FETD methods, T_m, B_m, $S_m\ge 0$, the stability condition is obviously satisfied when $\beta\ge 1/4$. On the other hand, matrix $\mathbf{S}$ in the EVFE formulation is no longer positive definite. Consequently, the stability condition is stricter. In order for the real part of z_m to be nonpositive, the following conditions must hold:

$$\begin{aligned}a&>0\\\mathrm{Re}(b)&\ge 0\\\mathrm{Re}\left(-b+\sqrt{b^2-4ac}\right)&\le 0.\end{aligned} \tag{20}$$

For arbitrary media, the first condition is satisfied only when $\beta=1/4$, while the second condition always holds. Therefore, the only task left is to prove that the third condition holds when $\beta=1/4$. This is achieved by rewriting the coefficient matrices

$$\begin{aligned}\mathbf{T}&=\frac{\mu_r}{c_0^2}\,\mathbf{Q}\\\mathbf{B}&=\frac{\mu_r}{c_0^2}\,(2j\omega_c+\alpha)\mathbf{Q}\\\mathbf{S}&=\frac{1}{\varepsilon_r}\,\mathbf{P}-\frac{\mu_r}{c_0^2}\,(\omega_c^2-j\alpha\omega_c)\mathbf{Q}\end{aligned} \tag{21}$$

where $\mathbf{P}$ is a semipositive definite matrix and $\mathbf{Q}$ is positive definite matrix. They are self-adjointing matrices defined by

$$\begin{aligned}P_{ij}&=\iint_s\nabla W_i\cdot\nabla W_j\cdot ds\\Q_{ij}&=\iint_s W_i\cdot W_j\cdot ds.\end{aligned} \tag{22}$$

Their inner products should have the same relationship as in (21). Substituting this relationship into (20) yields

$$\begin{aligned}&\mathrm{Re}\left(-b+\sqrt{b^2-4ac}\right)\\&\quad=\mathrm{Re}\left(-\frac{2\alpha\mu_r}{c_0^2}\,\Delta tQ_m\right.\\&\qquad\left.+\sqrt{\left(\frac{2\alpha\mu_r}{c_0^2}\,\Delta tQ_m\right)^2-16\,\frac{\mu_r\Delta t^2}{\varepsilon_rc_0^2}\,P_mQ_m}\right).\end{aligned} \tag{23}$$

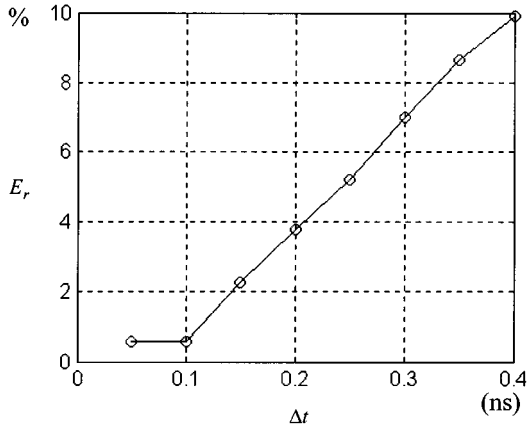

Fig. 1. Relative error of the resonant frequency in a 2-D cavity versus different widths of the time step. The exact resonant frequency is 3.0364 GHz.

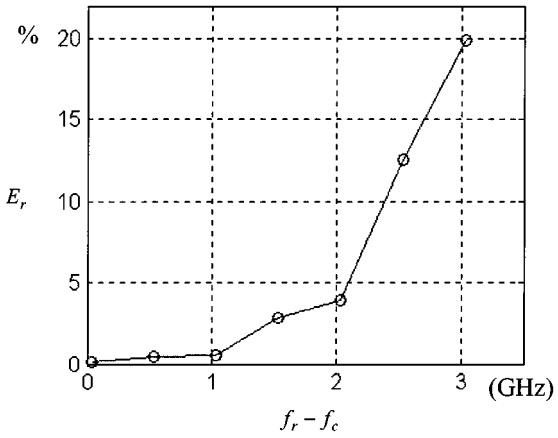

Fig. 2. Relative error of the resonant frequency in a 2-D cavity versus difference frequency between the resonance and the carrier. The exact resonant frequency is 3.0364 GHz.

Since $P_m \geq 0$ and $Q_m > 0$, it is easy to show that the above formula is nonpositive. Hence, $\beta = 1/4$ leads to an unconditionally stable EVFE update scheme.

IV. Numerical Dispersion Analysis

Dispersion errors exist in most of the time-domain techniques. The major part of the error is due to the inaccurate modeling of the sinusoidal behavior of the electromagnetic wave. Piecewise polynomial discretization in the time domain is normally not a good approximation to sinusoids unless very fine time-step or very high-order polynomials are used. However, it is expected that the dispersion error for EVFE techniques will be less serious than other time-domain approaches, since it models the slowly varying signal envelope rather than the fast oscillating original signal waveform. To validate this statement, the resonant frequency for a 2-D rectangular cavity is calculated and the error versus different time steps and carrier frequencies are studied. The cavity is enclosed by PEC and there is no dielectric filled. The length of the cavity is 4.94 cm, which gives the lowest resonant frequency f_r at 3.0364 GHz. The system is excited by some bandlimited noise and the resonant frequency is obtained by locating the peaks in the Fourier transform of the late time signal envelope. Define the relative error percentage as $Er = 100 \cdot |\tilde{f}_r - f_r/f_r|$, where $\tilde{f}_r$ is the calculated resonant frequency. Fig. 1 plots E_r versus different time-step widths when the carrier frequency is fixed to 2.0 GHz. As expected, the relative error of the frequency calculation is almost proportional to the time step. In Fig. 2, the time step Δt is fixed to 0.1 ns, and the relative error versus different selection of carrier is studied and plotted versus the frequency difference between the resonance and the carrier. The relative error shows a second-order dependency to $f_r - f_c$. It is noticed that the dispersion error reaches its maximum when $f_c = 0$, which is the case for the FETD method. Overall, we have $E_r \propto (f_r - f_c)^2 \Delta t$. Therefore, for the least dispersion error without compromising the computation efficiency, the carrier frequency should be selected to be as close as possible to the simulated frequency. When there is no *a prior* knowledge of the frequency characteristics of the simulated signal, the best choice would be half of the highest frequency that one wants to simulate.

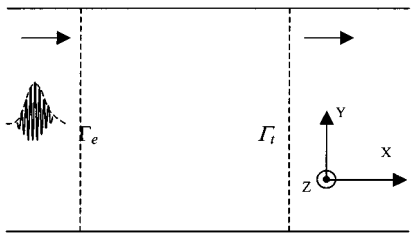

Fig. 3. Sketch of an empty planar waveguide.

V. Absorbing Boundary Conditions

Consider a general 2-D waveguide problem, where the path integral exists on the right-hand side of (5). As plotted in Fig. 3, the boundary Γ consists of PEC boundary Γ_c of the planar waveguide, excitation truncation boundary Γ_e, and the termination truncation boundary Γ_t. On PEC, Γ_c is a natural boundary condition and has no contribution to the right-hand side path integral. For the truncation boundaries, the Mur's first-order absorbing boundary condition (ABC) can be applied based on the traveling-wave assumption. In EVFE techniques, the frequency-domain version of ABC is always a good approximation to use if the signal bandwidth is relatively narrow. However, rigorous implementation of ABC in EVFE simulation requires special handling as follows. First let's consider the termination boundary Γ_t. The traveling wave assumption in the time domain is

$$\frac{\partial H_z}{\partial x} + \frac{1}{c_0}\frac{\partial H_z}{\partial t} = 0. \tag{24}$$

Substituting (3) into (24) leads to the envelope boundary condition

$$\frac{\partial V(t)}{\partial x} = -\frac{1}{c_0}\frac{\partial V(t)}{\partial t} - j\frac{\omega_c}{c_0}V(t). \tag{25}$$

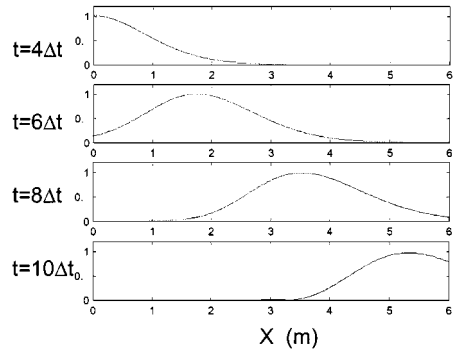

Fig. 4. Magnetic field envelope along the waveguide for different observation times.

The boundary condition for the excitation can be derived in a similar way as

$$\frac{\partial V(t)}{\partial x} = \frac{1}{c_0}\frac{\partial V(t)}{\partial t} + \frac{j\omega_c}{c_0}V(t) - \frac{2}{c_0}\frac{\partial V^i(t)}{\partial t} - \frac{2j\omega_c}{c_0}V^i(t) \tag{26}$$

where V^i is the envelope of incident field. Substituting (25) and (26) into the right-hand side path integral of (5) and rearranging both sides leads to the modification of the matrix coefficients in (6) as follows:

$$\begin{aligned}
\tilde{T}_{ij} &= T_{ij} \\
\tilde{B}_{ij} &= B_{ij} + \oint_{\Gamma} \frac{1}{c_0\varepsilon_r} W_i W_j \cdot dl \\
\tilde{S}_{ij} &= S_{ij} + \oint_{\Gamma} \frac{j\omega_c}{c_0\varepsilon_r} W_i W_j \cdot dl \\
\tilde{F}_i &= F_i + \oint_{\Gamma_e} \left[-\frac{2}{c\varepsilon_r}\frac{\partial v^i}{\partial t} - \frac{2j\omega_c}{c\varepsilon_r} v^i \right] \cdot W_i \, dl.
\end{aligned} \tag{27}$$

VI. Guided-Wave Numerical Examples

A couple of numerical examples are presented to validate the above formulations. The first example is an empty planar waveguide, depicted in Fig. 3. The waveguide is 6-m long and 4-cm wide. The incident wave is a modulated Gaussian pulse in the form of

$$H_z^i(t) = \exp\left[\frac{(t-3\sigma_t)^2}{2\sigma_t^2}\right] \bullet e^{j\omega_c t} \tag{28}$$

where $\omega_c = 2\pi f_c$, $f_c = 2.91$ GHz, and $\sigma_t = 3.0$ ns. For this excitation, the envelope/carrier frequency ratio is about 10%. Therefore, a time step $\Delta t = 1.5$ ns is used for the EVFE simulation, which is much wider than the carrier period. The total number of time steps used is 16. To get the same precision, an explicit FDTD method needs at least 200 times that and an implicit FETD simulation needs at least 20 times that. Since there is no discontinuity, the electromagnetic wave should propagate without dispersion. Fig. 4 plots the field envelope along the waveguide at different time steps, where a nice traveling wave effect is observed.

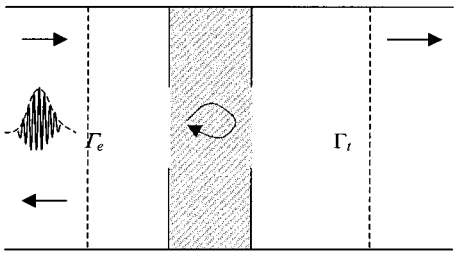

Fig. 5. Sketch of a planar waveguide with two debris, with or without dielectric filled in between.

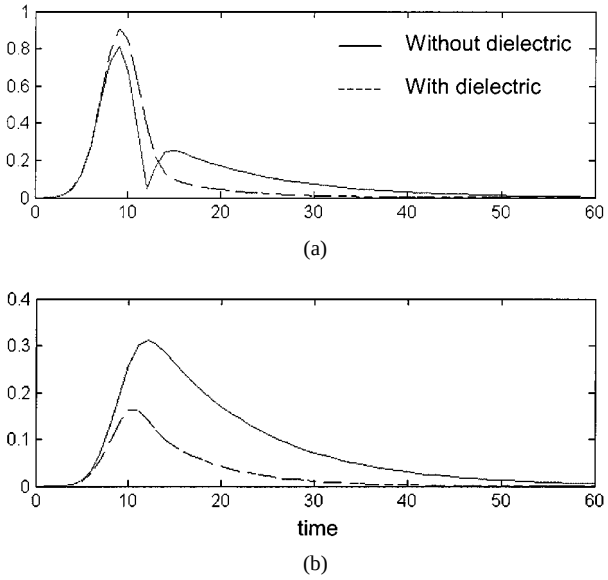

Fig. 6. Time-domain signal envelope for: (a) a return wave and (b) a through wave.

The second example is again the same planar waveguide, but with two irises in the middle. As depicted in Fig. 5, the length of the iris is 1.5 cm on each side. The two apertures are constructed 5 cm away from each other to intentionally form a resonance peak around the carrier frequency. The space between the two irises is filled either with or without dielectric. The same excitation and time step as in the first example are used. After the simulation, the time-domain signal envelope is recorded in both the excitation plane and the termination plane. The total number of time steps is 60. As shown in Fig. 6, the long tails of the signals are observed in both the return wave and through wave when there is no dielectric filled in between, which indicates a sharp frequency resonance. When the center is filled by lossy dielectric ($\varepsilon_r = 1.05$, $\sigma = 8.49 \times 10^{-4}$), it can be seen that the signal tails are much shortened, which represents the resonance is attenuated. By applying the Fourier transform to the time-domain waveform, the S-parameters are generated and plotted in Figs. 7 and 8 against the frequency-domain FEM results. Very good agreement is found from those comparisons, which further validates the approach. It is also noticed that the resonance peaks in the S-parameters are both shifted and weakened when lossy dielectric is filled in between.

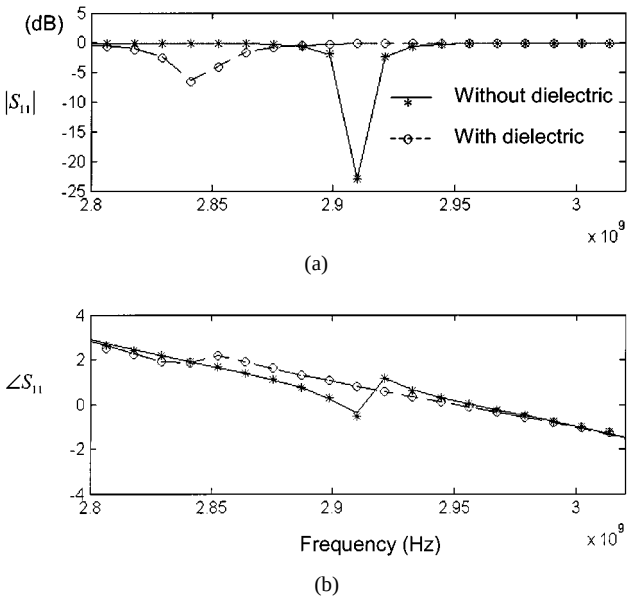

Fig. 7. Comparison of S_{11} between EVFE result (lines) and frequency-domain FEM result (signs). (a) Magnitude of S_{11}. (b) Phase of S_{11}.

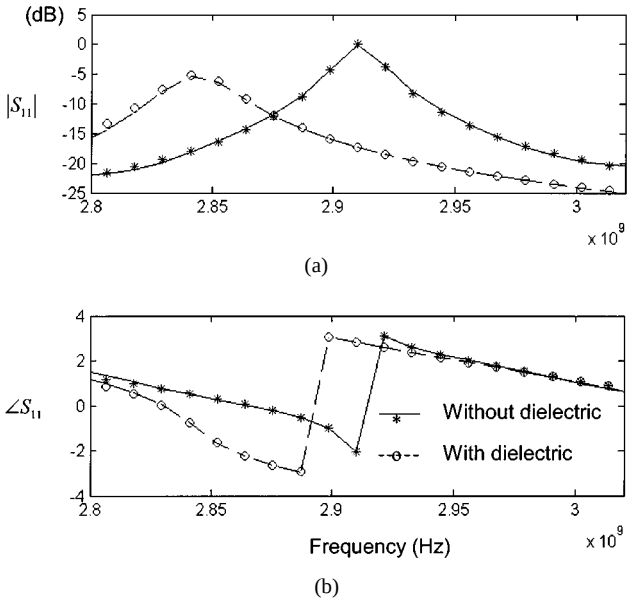

Fig. 8. Comparison of S_{21} between EVFE result (lines) and frequency-domain FEM result (signs). (a) Magnitude of S_{21}. (b) Phase of S_{21}.

VII. Conclusion

A novel full-wave electromagnetic simulation method called the EVFE technique has been proposed based on the envelope simulation concept. When applied to cases with athe slowly varying signal envelope on top of a fast oscillating carrier, it can reduce computation time over the traditional time-domain techniques. The approach has proven to be unconditionally stable. It has also been shown that EVFE techniques have generally better dispersion-error performance compared to FETD methods. Two 2-D numerical examples have been presented to validate the approach. Overall, EVFE can be considered as a more general electromagnetic simulation frame that unites the frequency-domain and time-domain techniques, since it reduces to frequency-domain FEM when the envelope is constant and to FETD when the carrier frequency is chosen to be zero.

References

[1] X. Zhang, J. Fang, K. K. Mei, and Y. Liu, "Calculations of the dispersive characteristics of microstrips by the time-domain finite difference method," *IEEE Trans. Microwave Theory Tech.*, vol. 36, pp. 263–267, Feb. 1988.

[2] Y. Hua and T. K. Sarkar, "Generalized pencil-of-function method for extracting poles of an EM system from its transient response," *IEEE Trans. Antennas Propagat.*, vol. 37, pp. 229–234, Feb. 1989.

[3] C.-N. Kuo, B. Houshmand, and T. Itoh, "Full-wave analysis of packaged microwave circuits with active and nonlinear devices: An FDTD approach," *IEEE Trans. Microwave Theory Tech.*, vol. 45, pp. 819–826, May 1997.

[4] S.-H. Chang, R. Coccioli, Y. Qian, and T. Itoh, "A global finite-element time-domain analysis of active nonlinear microwave circuits," *IEEE Trans. Microwave Theory Tech.*, vol. 47, pp. 2410–2416, Dec. 1999.

[5] S. D. Gedney and U. Navsariwala, "An unconditionally stable finite element time-domain solution of the vector wave equation," *IEEE Microwave Guided Wave Lett.*, vol. 5, pp. 332–334, Oct. 1995.

[6] J. F. Lee, R. Lee, and A. Cangellaris, "Time-domain finite-element methods," *IEEE Trans. Antennas Propagat.*, vol. 45, no. 3, pp. 430–442, March 1997.

[7] H. S. Yap, "Designing to digital wireless specifications using circuit envelope simulation," in *Asia–Pacific Microwave Conf.*, 1997, pp. 173–176.

[8] J. L. Volakis, A. Chatterjee, and L. C. Kempel, *Finite Element Method for Electromagnetics*. Piscataway, NJ: IEEE Press, 1998.

[9] I. Gohberg, P. Lancaster, and L. Rodman, *Matrix Polynomials*. New York: Academic, 1992.

Yuanxun Wang (S'96–M'99) was born in Hubei, China, in 1973. He received the B.S. degree in electrical engineering from the University of Science and Technology of China (USTC), Hefei, China, in 1993, and the M.S. and Ph.D. degrees in electrical engineering from The University of Texas at Austin, in 1996 and 1999, respectively.

From 1995 to 1999, he was a Research Assistant in the Department of Electrical and Computer Engineering, The University of Texas at Austin. In 1999, he joined the Department of Electrical Engineering, University of California at Los Angeles, where he is currently a Research Engineer and Lecturer. His research interests are on the enabling technology for RF and microwave front-ends in wireless communication and radar systems, as well as the numerical modeling, simulation, and feature extraction techniques for microwave circuits, antennas, and electromagnetic scattering. He has authored or co-authored approximately 40 refereed journal and conference papers.

Tatsuo Itoh (S'69–M'69–SM'74–F'82) received the Ph.D. degree in electrical engineering from the University of Illinois at Urbana-Champaign, in 1969.

From September 1966 to April 1976, he was with the Electrical Engineering Department, University of Illinois at Urbana-Champaign. From April 1976 to August 1977, he was a Senior Research Engineer in the Radio Physics Laboratory, SRI International, Menlo Park, CA. From August 1977 to June 1978, he was an Associate Professor at the University of Kentucky, Lexington. In July 1978, he joined the faculty at The University of Texas at Austin, where he became a Professor of electrical engineering in 1981 and Director of the Electrical Engineering Research Laboratory in 1984. During the summer of 1979, he was a Guest Researcher at AEG-Telefunken, Ulm, Germany. In September 1983, he was selected to hold the Hayden Head Centennial Professorship of Engineering at The University of Texas at Austin. In September 1984, he was appointed

Associate Chairman for Research and Planning of the Electrical and Computer Engineering Department, The University of Texas. In January 1991, he joined the University of California at Los Angeles, as Professor of Electrical Engineering and Holder of the TRW Endowed Chair in Microwave and Millimeter Wave Electronics. He was an Honorary Visiting Professor at the Nanjing Institute of Technology, Nanjing, China, and at the Japan Defense Academy. In April 1994, he was appointed as Adjunct Research Officer for the Communications Research Laboratory, Ministry of Post and Telecommunication, Japan. He currently holds a Visiting Professorship at The University of Leeds, Leeds, U.K., and is an External Examiner of the Graduate Program of the City University of Hong Kong. He has authored or co–authored 280 journal publications, 585 refereed conference presentations, and has written 30 books/book chapters in the area of microwaves, millimeter-waves, antennas and numerical electromagnetics. He has overseen 49 Ph.D. students.

Dr. Itoh is a member of the Institute of Electronics and Communication Engineers of Japan and Commissions B and D of USNC/URSI. He has been the recipient of numerous awards including the Shida Award presented by the Japanese Ministry of Post and Telecommunications in 1998, the Japan Microwave Prize in 1998, the IEEE Third Millennium Medal in 2000, and the IEEE Microwave Theory and Techniques Society (IEEE MTT-S) Distinguished Educator Award in 2000. He served as the editor of the IEEE TRANSACTIONS ON MICROWAVE THEORY AND TECHNIQUES from 1983 to 1985. He serves on the Administrative Committee of the IEEE MTT-S. He was vice president of the IEEE MTT-S in 1989 and president in 1990. He was the editor-in-chief of IEEE MICROWAVE AND GUIDED WAVE LETTERS from 1991 through 1994. He was elected as an Honorary Life Member of the MTT-S in 1994. He was the chairman of the USNC/URSI Commission D from 1988 to 1990, and chairman of Commission D of the International URSI from 1993 to 1996. He is chair of the Long Range Planning Committee of the URSI. He also serves on advisory boards and committees of a number of organizations.